Title

Simultaneous two color image capture for sub-diffraction localization fluorescence microscopy

Authors

Glasgow, Ben J
Ma, Lie

Publication Date

2016

DOI

10.1016/j.micron.2015.09.007

Peer reviewed

HHS Public Access

Author manuscript

Micron. Author manuscript; available in PMC 2017 January 01.

Published in final edited form as:

Micron. 2016 January ; 80: 14–19. doi:10.1016/j.micron.2015.09.007.

Simultaneous Two Color Image Capture for Sub-diffraction Localization Fluorescence Microscopy

Ben J. Glasgow[*] and **Lie Ma**

Departments of Ophthalmology, Pathology and Laboratory Medicine, Jules Stein Eye Institute, University of California, Los Angeles, 100 Stein Plaza Rm. BH 623, Los Angeles, CA 90095

Abstract

A sub-diffraction limit fluorescence localization microscope was constructed using a standard cooled 1.4 mega-pixel fluorescence charge-coupled device (CCD) camera to simultaneously resolve closely adjacent paired quantum dots on a flat surface with emissions of 540 and 630 nm. The images of the overlapping Airy discs were analyzed to determine the center of the point spread function after noise reduction using Fourier transformation analysis. The Cartesian coordinates of the centers of the point spread functions were compared in serial images. Histograms constructed from serial images fit well to Gaussian functions for resolving two quantum dots separated by as little as 10 nm in the x-y coordinates. Statistical analysis of multiple pairs validated discrimination of inter-fluorophore distances that vary by 10 nm. The method is simple and developed for x-y resolution of dilute fluorophores on a flat surface, not serial z sectioning.

Keywords

Super-resolution microscopy; Diffraction unlimited; Fluorescence; Localization Microscopy; Quantum dots; CCD camera

1.0 Introduction

Advances in fluorescence microscopy have enabled resolution of distances beneath the light diffraction limit. After confocal laser scanning microscopy (Cremer and Cremer, 1978), resolution improved with illumination techniques that exploited evanescence of light in total internal reflectance fluorescence (TIRF) (Axelrod, 1981), and scanning near field optical microscopy (SNOM) (Betzig et al., 1991). Standing light waves were used in structured illumination microscopy (SIM) (Bailey et al., 1993). Non-linear responses of fluorophores have been harnessed in other techniques such as stimulated emission depletion microscopy (STED) (Hell and Wichmann, 1994).

[*]Corresponding author at: David Geffen UCLA School of Medicine, Departments of Ophthalmology, Pathology and Laboratory Medicine, Jules Stein Eye Institute, 100 Stein Plaza, BH 632, Los Angeles, CA 90095-, United States. bglasgow@mednet.ucla.edu (BJ Glasgow).

Methods that use the point spread function of fluorescence emission to position emitters are referred to as localization microscopy. For photons emitted from the same source, the center of the point spread function reflects the photon probability distribution and is estimated more accurately than the width of the beam that is determined by photon position (Agard and Sedat, 1983). Variations of these techniques allow sequential isolation of emissions separated in time and space (e.g. confocal microscopy (Bornfleth et al., 1998), photoactivated localization microscopy (PALM) (Betzig et al., 2006), fluorescence photoactivation localization microscopy (FPALM) (Hess Girirajan T, Mason M, 2006) (Hess et al., 2009), stochastic optical reconstruction microscopy (STORM) (Rust et al., 2006). A comparison of techniques shows an approximate resolution in the x-y plane in images of about 20 nanometers (Schermelleh et al., 2010). Generally, the instruments to achieve “super-resolution” are expensive and remain out of the reach of the average researcher. Yet many applications require only the determination of distance between fluorophores in one plane. Because of the pioneering work in many disciplines, resolution predicated only on the Gaussian fit of the point spread function and the number of photons detected can be hypothetically realized with inexpensive lasers, robust single point emitters (e.g. quantum dots), CCD cameras and commonplace computer software. Noise reduction is now routine by Fourier transformation and can further improve the image quality. Use of simultaneous two color image capture and discrimination of different fluorophores potentially could eliminate the effects of motion and obviate the need for registration or fiducials for images collected separated either in time or space. With the goal of simplicity we assembled an uncomplicated microscope and camera of modest resolution to test nanoscale precision potentially accessible by virtually all laboratories.

2 Materials and Methods

2.1 Microscope

The home built microscope is shown in Figure 1. The excitation source, a 405 nm, 150 mW, diode laser (Thorlabs, Inc.), 3.8 mm beam diameter, is driven by a 250 mA blue laser diode drive board (Thorlabs, Inc.). Transmitted light is focused into a multimode fiber optic patch cable (Thorlabs, Inc.) and the beam is reflected with a 409 nm 25 × 36 mm Bright line single edge dichroic (Semrock, Inc.) and focused with a 1.4 numerical aperture 100x objective lens (Carl Zeiss, A.G., 440780-9904). Glass slides are mounted to the stage on a hollow aluminum cylinder that is secured with a through bolt to minimize motion. The samples may be viewed from above or from the side by shifting the position of the stage. Stage movement is facilitated with 3 axis adjustment micrometers (Mitutoyo Corp and Newport Corp.). The focal length is adjusted with a differential actuator (1/2” manual drive with .5 μM graduated lockable thumbscrews (Thorlabs, Inc.). Emitted light passes through a 500 nm cutoff long pass filter FEH 0500 (Thorlabs, Inc.) enabling red and green to be visualized simultaneously. Emitted light is captured with 1.4 MP Nikon DS-Ri1 camera, Peltier cooled to −10 degrees. Exposure time at 80 msec provides optimal image quality while preserving sample integrity. The diode laser is controlled and synchronized to the corresponding exposure period. The pixel size is 55 nm.

2.2 Samples Preparation

Six nanometer diameter CdSeS/ZnS alloyed quantum dots (Sigma-Aldrich Co.) with emission maxima of 540 and 630 μm were diluted 1:2500 in a solution of toluene and 3 μl were dried on a 22 × 22 mm cover glass of 170μm thickness. Multiple frames of the same field were recorded and later analyzed to spatially resolve overlapping quantum dots of different colors.

2.3 Image Analysis

Raw images were recorded as 16 bit RGB tiff files and analyzed in Matlab (MathWorks, Inc.) according to the algorithm in Figure 2. The program was instructed to separate bright spots from background using global gray scale threshold regions, which correspond to the Airy discs of closely paired red and green fluorophores. The regions of interest around the Airy discs were restricted to the presence of both green and red colors in the bright spots of the original image. Noise reduction was performed on the designated spots by Fourier transform (Figure 3). A filter mask was placed around the central area of the Fourier transformed image to eliminate high frequency noise. Finally, an inverse Fourier transform recovered the real image from Fourier space. The centers of the point spread function of the paired fluorophores were transposed to Cartesian coordinates using the same frame of reference and the program was instructed to calculate the inter-fluorophore distances for all green and red quantum pairs in each image. The de-noised intensity data from red and green color channels were then fitted to a two dimensional Gaussian formula by least-squares analysis:

$$equ \quad A1 \quad \mathrm{f}(\mathrm{x},\mathrm{y}) = A exp\left(-\left((\mathrm{x}-\mathrm{x_o})^2/2\sigma^2\right)+(\mathrm{y}-\mathrm{y_0})^2/2\sigma^2\right)+\mathrm{z_o}$$

where A is the amplitude or intensity, x_o,y_o is the center, σ is the standard deviation, z_o.is an offset constant.

In order to evaluate the statistical properties of calculated distances between quantum dots for each pair set, histograms of pair distances were fit to a standard Gaussian equation for analysis:

$$equ \quad A2 \quad \mathrm{f}(\mathrm{x}) = A exp\left(-\left(\left(\mathrm{x}-{\mathrm{x_o}}^2/2\sigma^2\right)\right)\right)+\mathrm{z_o} \quad \text{with the same parameters as equ A1.}$$

The coefficient of determination (R2) was calculated:

$$\text{equ A3} \quad R2 = 1 - \text{residual sum of squares/total sum of squares.}$$

2.4 To assess the fidelity with which the method discriminates various inter-fluorophore distances, the normalized probability distribution functions were compared. To assess discriminating potential, the ANOVA test statistic was used to determine if the means of

distances between fluorophore distances were significantly different from one another for various putative distances.

3. Results and Discussion

3.1. Resolution

According to Abbe's law the resolved distance (d) between fluorophores in a light microscope is limited by the wavelength (λ) and numerical aperture (NA) of the lens:

$$equ \quad \text{A4} \quad \text{d}=\lambda/2\,(NA)$$

(Abbe, 1873)

For an emission at 630 nm the diffraction limited resolution is about 225 nm. Histograms were constructed from multiple repeatedly captured images without moving the stage. Figure 3 shows the Gaussian fitting results for the distance between the centers of the point spread functions of two fluorophores. The number of images recorded varied between 25 to over 500. Despite the relatively low number of images, fluorophores separated by distances greater than 10 nm gave consistent Gaussian fitting with R^2 values approaching unity. (Figure 4). In general the greater the separation, the better the Gaussian fit. An R^2 value greater than .94 was returned for overlapping fluorophores that were extremely close ~9 nm. This is only an estimate because the Gaussian function is obviously skewed to the left. The differences in some calculated inter-fluorophore distances in this set were less than the theoretical separation of quantum dots that are 6 nm in diameter. For statistical evaluation, the median value probably is a more realistic value (9 nm) than the fitted mean (6 nm). Therefore, an additional calculation was performed using the median value but the variance was preserved. The statistical tests with and without this alteration showed that separations greater than 10 nm were still significantly different from one another (Table 1). However, the method failed to distinguish areas between pairs less than 5 nm (red highlighted p values in Table 1 because the overlap is too great. The means and standard deviations of the inter-fluorophore distances are plotted (Figure 5). The data were consistent despite the inevitable non-constant drift generated between the camera and coverslip that occurs in every microscope. Noise reduction is critical to obtaining these data and easily gained from standard Fourier transformation for image analysis (Figure 3).

3.2. Normalized Probability Distribution Function

The discrimination of intermolecular distances between fluorophore pairs is necessary to validate the utility of this method. For our future application the compartment size requires the ability to differentiate intermolecular distances of ≤40 nm. Figure 6 shows the normalized probability distribution functions of each fluorophore pair to show the discrimination between inter-fluorophore distances derived from the center of the fitted Gaussian functions.. The distributions show wide standard deviations but the means are segregated in most cases. A pair of fluorophores separated by 10 nm is easily distinguished with no overlap from a pair separated by 40 nm. The ANOVA confirms that the means are

significantly different for most sets (Tables 1) despite the wide standard deviation. Collection of more images would probably reduce the overlap.

3.3 Advantages

3.31. Colored CCD camera—Simultaneously collection of two colors in images averts the need for two detectors and the error associated with alignment of optics or images. Commercial colored CCD cameras are relatively inexpensive and usually have optimized image software. The CCD not only reduces the overall cost of equipment but also permits the ability to use the same reference frame for both color channels. Distance discrimination is then possible with application of a simple distance formula for the calculations of regions in the same reference frame. In addition there is no need for scanning as the regions of interest are collected in each frame.

3.32. Center of the point spread function—Estimation of the center of intensity of the point spread function is known to be more accurate than estimation of the width for single fluorophores (Thompson et al., 2002) (Pertsinidis et al., 2010). The increased sensitivity in newer CCD cameras and extended integration times facilitate the signal. Combined with rapid analysis from inexpensive and widely used software (such as Matlab), the determination of the centers of the point spread functions and inter-fluorophore distances is facilitated. The method is computationally and technologically less intensive than other techniques (e.g. SIM, STED or STORM).

3.4. Limitations

This application of localization microscopy was tested for only pairs of quantum dots of different colors to provide distance measurements. The precision of the method is improved by taking multiple images with isolated bright fluorophores and constructing a histogram in which measured distance measurements are binned and then fit to a Gaussian function. The goal to discriminate inter-fluorophore distances between proximal sets of fluorophores (i.e. 40 nm versus 10 nm) was accomplished. Figures 5, 6 and Tables 1 show that differences in distances as little as 10 nm can be measured reliably. One drawback of the method is the need for multiple images taken within the time limits of fluorophore bleaching. The effects of photobleaching and fluorophore stability were largely circumvented in the study design by using robust quantum dots as proof of concept. Fluorescence dyes are as yet untested in this system. Obviously the system currently is best for sparse concentration of robust fluorophores and is ideal for applications where the fluorophore density can be controlled. Localization with distance measurement between 2 molecules each of which is labeled with a unique color to test their relationship within cellular organelles may be achievable by our system. This method would potentially work very well in very thin sections (Parfitt et al., 2012). The implementation of photoswitchable dyes such as Cy 5 has been applied in simple applications to achieve 38 nm FWHM resolution (Yuan et al., 2014). Subnanometer resolution has been gained using these dyes in tandem with active feedback stabilization (Pertsinidis et al., 2010). Photoswitchable dyes applied in our simple method might permit imaging of more dense overlapping multi-colored fluorophores.

4. Conclusions

The method described here was tested with quantum dots that are excited over a broad spectra range, resistant to bleaching, and analyzed in one plane. This sort of approach is best applied in sections where only x and y coordinates are relevant and compartmentalization between 2 fluorophores of different colors is being tested. Resolution can be attained for two fluorophores separated by as little as 10 nm. This method is best suited to discriminate a difference in inter-fluorophore distances in any particular compartment by at least 10 nm and should be applicable to localization in organelles. The instruments and software needed to gain nanometer resolution are within the reach of small research laboratories.

Acknowledgements

This work was supported by Public Health Service grant EY 11224 from the National Eye Institute (BG), and EY 00331 (Institute Core) and the Edith and Lew Wasserman Endowed Professorship (BG)

References

Abbe E. Beiträge zur Theorie des Mikroskops und der mikroskopischen Wahrnehmung. Arch. für Mikroskopische Anat. 1873 doi:10.1007/BF02956173.

Agard DA, Sedat JW. Three-dimensional architecture of a polytene nucleus. Nature. 1983; 302:676–681. doi:10.1038/302676a0. [PubMed: 6403872]

Axelrod D. Cell-substrate contacts illuminated by total internal reflection fluorescence. J. Cell Biol. 1981; 89:141–145. doi:10.1083/jcb.89.1.141. [PubMed: 7014571]

Bailey B, Farkas DL, Taylor DL, Lanni F. Enhancement of axial resolution in fluorescence microscopy by standing-wave excitation. Nature. 1993; 366:44–48. doi:10.1038/366044a0. [PubMed: 8232536]

Betzig E, Patterson GH, Sougrat R, Lindwasser OW, Olenych S, Bonifacino JS, Davidson MW, Lippincott-Schwartz J, Hess HF. Imaging intracellular fluorescent proteins at nanometer resolution. Science. 2006; 313:1642–1645. doi:10.1126/science.1127344. [PubMed: 16902090]

Betzig E, Trautman JK, Harris TD, Weiner JS, Kostelak RL. Breaking the diffraction barrier: optical microscopy on a nanometric scale. Science. 1991; 251:1468–1470. doi:10.1126/science.251.5000.1468. [PubMed: 17779440]

Bornfleth H, Sätzler K, Eils R, Cremer C. High-precision distance measurements and volume-conserving segmentation of objects near and below the resolution limit in three-dimensional confocal fluorescence microscopy. J. Microsc. 1998; 189:118–136. doi:10.1046/j.1365-2818.1998.00276.x.

Cremer C, Cremer T. Considerations on a laser-scanning-microscope with high resolution and depth of field. Microsc. Acta. 1978; 81:31–44. [PubMed: 713859]

Hell SW, Wichmann J. Breaking the diffraction resolution limit by stimulated emission: stimulated emission depletion microscopy. Opt. Lett. 1994; 19:780–782. [PubMed: 19844443]

Hess Girirajan T, Mason M S. Ultra-High Resoluion Imaging by Fluorescence Photoactivation Localization Microscopy. Biophys. J. 2006; 91:4258–4272. doi:10.1529/biophysj.106.091116. [PubMed: 16980368]

Hess ST, Gould TJ, Gunewardene M, Bewersdorf J, Mason MD. Ultrahigh resolution imaging of biomolecules by fluorescence photoactivation localization microscopy. Methods Mol. Biol. 2009; 544:483–522. doi:10.1007/978-1-59745-483-4_32. [PubMed: 19488720]

Parfitt GJ, Xie Y, Reid KM, Dervillez X, Brown DJ, Jester JV. A novel immunofluorescent computed tomography (ICT) method to localise and quantify multiple antigens in large tissue volumes at high resolution. PLoS One. 2012; 7:e53245. doi:10.1371/journal.pone.0053245. [PubMed: 23300899]

Pertsinidis A, Zhang Y, Chu S. Subnanometre single-molecule localization, registration and distance measurements. Nature. 2010; 466:647–651. doi:10.1038/nature09163. [PubMed: 20613725]

Rust MJ, Bates M, Zhuang X. Sub-diffraction-limit imaging by stochastic optical reconstruction microscopy (STORM). Nat. Methods. 2006; 3:793–5. doi:10.1038/nmeth929. [PubMed: 16896339]

Schermelleh L, Heintzmann R, Leonhardt H. A guide to super-resolution fluorescence microscopy. J. Cell Biol. 2010 doi:10.1083/jcb.201002018.

Thompson RE, Larson DR, Webb WW. Precise nanometer localization analysis for individual fluorescent probes. Biophys. J. 2002; 82:2775–83. doi:10.1016/S0006-3495(02)75618-X. [PubMed: 11964263]

Yuan Z, Sun J, Zhai R, Li X, Shao Z. Mercury arc lamp based super-resolution imaging with conventional fluorescence microscopes. Micron. 2014; 59:24–7. doi:10.1016/j.micron.2013.11.006. [PubMed: 24530361]

Highlights

-Diffraction unlimited microscopy performed economically with a CCD.

-Image processing facilitated by widely available software.

-Distance calculations are simplified in the same reference frame.

-10 nm separation of fluorophores was resolved from analysis of the point spread functions.

-Applicable for discriminating paired inter-fluorophore distances in planar configuration.

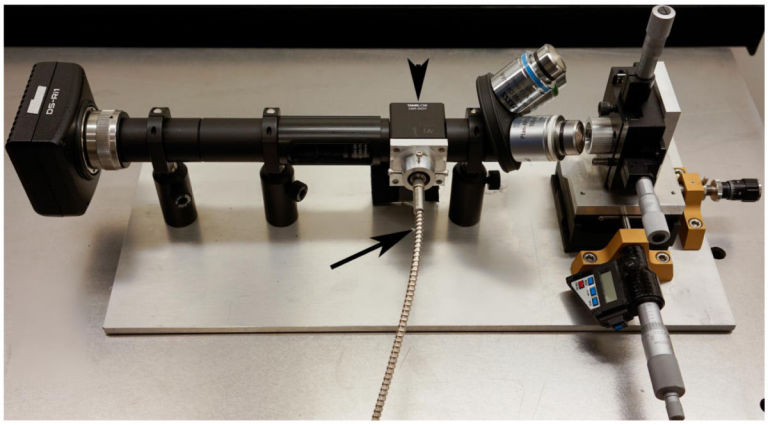

Figure 1.

Microscope for simultaneous 2 color capture localization is shown on an air table. From the left a black CCD camera is connected to a tube containing a focusing lens. The dichroic mirror and filters (arrowhead) are attached to the multimode fiber laser input (arrow). The objects and stage are shown at the far right.

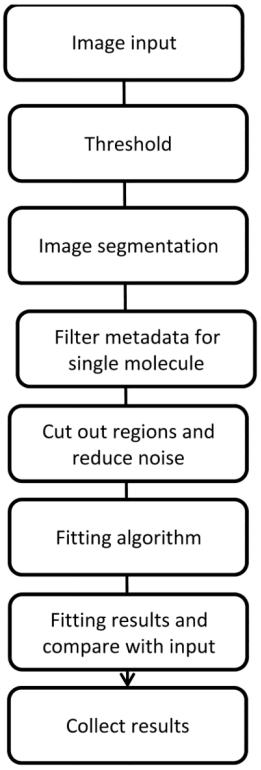

Figure 2.
Algorithm for image analysis from top to bottom.

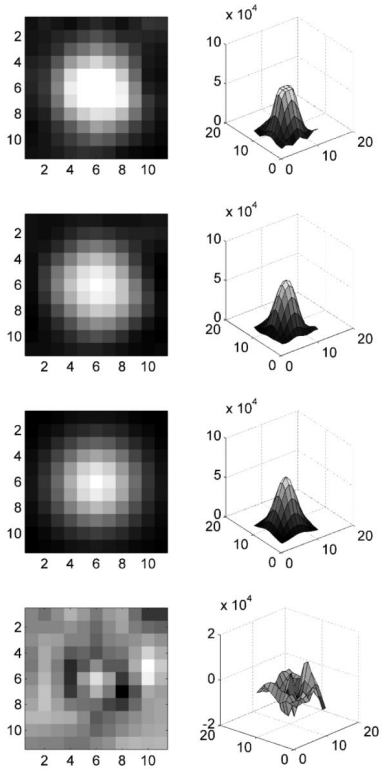

Figure 3.

Example of noise reduction from (a) the image after color (green or red) separation in gray scale followed by (b) constraints to the central area for the application of a filter mask to reduce high frequency noise, (c) the image recovered by the inverse Fourier transform and (d) the noise that was removed by the Fourier transform. Pixel numbers are given on the x and y axes.

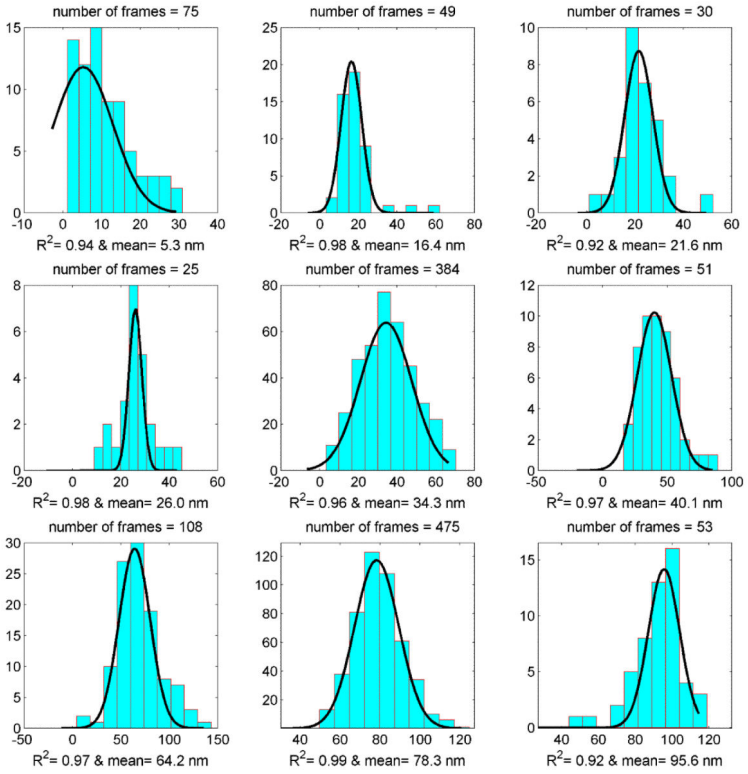

Figure 4.

Gaussian fittings of the histograms for inter-fluorophore distances for paired adjacent red and green quantum dots. The number of images to build the corresponding histograms are shown for each at the top and R^2 values (coefficients of determination) and mean distance of separation shown at the bottom of each histogram.

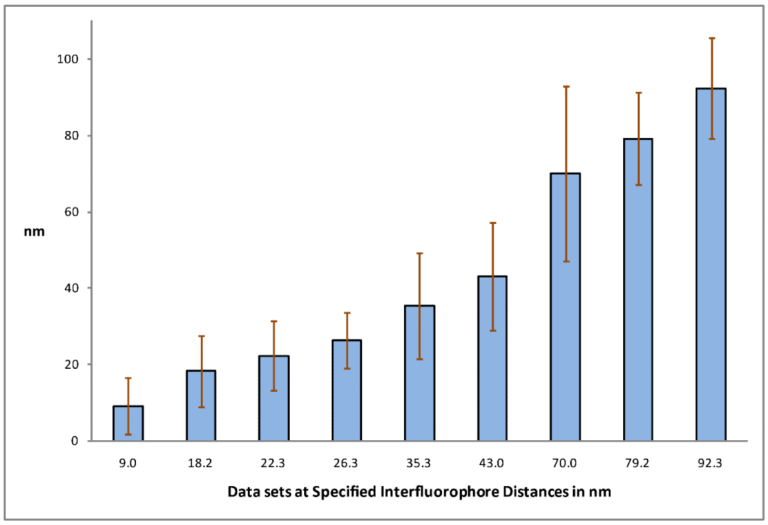

Figure 5.

Mean and standard deviations of inter-fluorophore distances for red-green quantum dot paired data sets. The inter-fluorophore distance at 9 nm is the median to realistically account for the skewed Gaussian (Figure 4). The variance from the Gaussian fit is retained.

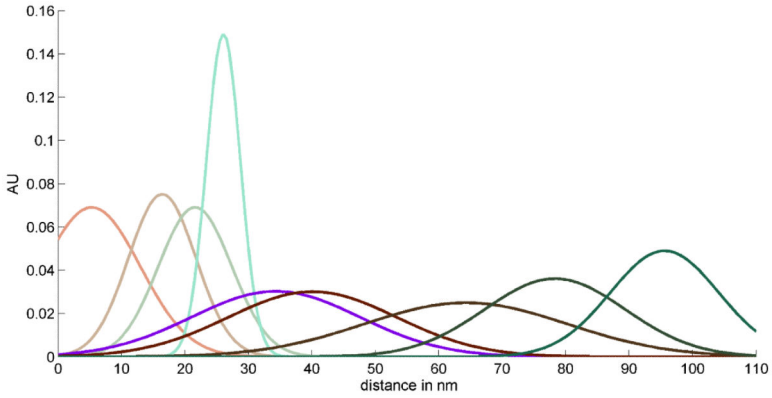

Figure 6.

Probability distribution function normalized by area under the curve for inter-fluorophore distances of red-green quantum dot pair to show relative discrimination of the sets.

Table 1

Comparison of means of inter-fluorophore distances (Anova test p values)

index/distance (nm)	9	16.4	21.6	26	34.3	40.1	64.2	78.3	95.6
9		<.001	<.001	<.001	<.001	<.001	<.001	<.001	<.001
16.4			0.06	<.001	<.001	<.001	<.001	<.001	<.001
21.6				0.09	<.001	<.001	<.001	<.001	<.001
26					<0.005	<.001	<.001	<.001	<.001
34.3						<.001	<.001	<.001	<.001
40.1							<.001	<.001	<.001
64.2								<.001	<.001
78.3									<.001